Available online at www.sciencedirect.com
ScienceDirect
ELSEVIER
Microelectronic Engineering 84 (2007) 1585–1588
MICROELECTRONIC ENGINEERING
www.elsevier.com/locate/mee

Fabrication and transport of large-scale molecular tunnel-junction arrays

Giuseppe Maruccio *, Pasquale Marzo, Roman Krahne, Antonio Della Torre, Adriana Passaseo, Roberto Cingolani, Ross Rinaldi

National Nanotechnology Laboratory of CNR-INFM, University of Lecce, Via per Arnesano, 73100 Lecce, Italy

Available online 1 February 2007

Abstract

We demonstrate a method for the simultaneous fabrication (without the need of expensive e-beam systems) of large arrays of nanodevices working at room temperature. The electrode gap is defined by a selective wet-etching of a AlGaAs/GaAs quantum well structure and controlled with nanometer precision. A selective oxidation of the Al rich barrier reduces the bulk leakage current by six orders of magnitude and extends the applicability of the produced devices to room temperature functionality. As a demonstration, we employ here these nanojunctions to investigate transport in molecular tunnel-junctions based on individual Azurins, a blue copper protein, under ambient conditions. This approach opens the way to the fabrication of complex circuits consisting of different nanodevices.
© 2007 Elsevier B.V. All rights reserved.

Keywords: Nanotechnology; Molecular electronics; Nanofabrication; Nanoelectronics; Lithography

1. Introduction

Molecular electronics [1] is aimed at building complex and functional devices based on few/single molecules. As a proof of concept, a number of individual components [2–7] has been reported, revealing intriguing features such as rectification [8,9], negative differential resistance [10] and Kondo effect [3,11,12]. Moreover, logic circuits based on CNT or nanowires have been also demonstrated. However, the economic fabrication of complex molecular electronics circuits on a large scale is still a major challenge, due to the difficulties in interconnecting molecules and fabricating electrical contacts to the outside world.

In the last years, different techniques (including mechanical break junctions, electron beam lithography, electromigration, electrodeposition, etc.) have been developed for patterning at the nanometer scale, beyond the intrinsic physical limitations of optical lithography. However, none of these methods equals the advantages of photolithography for low cost and high throughput and most of the proposed methods are appropriate for contacting single devices only. Thus, a major requirement in the establishment of molecular electronics consists in the demonstration of reproducible and economic methods for the fabrication of large-scale arrays of nanojunctions/nanodevices.

Recently, the fabrication of a large array of nanojunctions by optical lithography and wet etching of an AlGaAs/GaAs quantum-well (QW) structure has been reported by Krahne et al. [13]. The main advantage in this method is that the thickness of the quantum well and of the deposited metal layer controls the nanogap size with subnanometer precision, without the need of expensive e-beam systems. However, this innovative approach to nanoscale electronics has some intrinsic drawbacks: because of the bulk leakage currents through the semiconductor substrate under ambient conditions, such nanojunctions can be employed at cryogenic temperatures and in the dark only.

In this work, we significantly improve this method by means of selective oxidation of the two AlGaAs barriers above and below the QW in order to reduce the leakage current through the semiconductor layers and thus extend

* Corresponding author. Tel.: +39 0832 298211; fax: +39 0832 298180. *E-mail address:* giuseppe.maruccio@unile.it (G. Maruccio).

0167-9317/$ - see front matter © 2007 Elsevier B.V. All rights reserved.
doi:10.1016/j.mee.2007.01.107

the functionality of these nano-scaled devices to room temperature. As a demonstration of their use, we employ the fabricated nanojunctions to study, under ambient conditions and at the single-molecule level, electrical transport in Azurin (a small blue copper protein) immobilized between the electrodes. Typical molecular features, such as negative differential resistance (NDR), are observed in the *I*–*V* characteristics.

2. Fabrication process

First, an AlGaAs/GaAs quantum-well structure on a GaAs substrate is grown in a horizontal low pressure MOCVD system (AIXTRON 200 AIX). The layer sequence consists of a 200-nm-thick GaAs buffer layer, a 300-nm-thick $Al_xGa_{1-x}As$ lower barrier-layer, a 20 nm GaAs quantum well, a 100-nm-thick $Al_xGa_{1-x}As$ upper barrier-layer and a 10-nm-thick GaAs cap layer, which terminates the structure. All layers are undoped and grown at 750 °C. The thickness of the embedded GaAs layer was varied between 15 and 20 nm in various samples, while the Al concentration in the two AlGaAs barriers above and below the QW was varied between 35% and 90%.

After cleaning with acetone and isopropanol, 250 nm-high mesa structures were defined by means of a combination of optical lithography (AZ5214E photoresist, Karl Suss MJB3 mask aligner) and standard wet-etching carried out in $H_2O/H_2O_2/H_2PO_4$ with a ratio of 50:1:1 for 120 s at 24 °C. Crystal facets define the slope and the mesa structures exhibit sloped edges where the GaAs layer is exposed (Fig. 1c). Then, we employed a selective wet etching (in a solution of citric acid and H_2O_2 5:1) to remove a few tens of nanometers of the GaAs layer from the sloped edges of the mesa (Fig. 1c). As a result, a nanogap is formed exactly where the GaAs was removed (Fig. 1c) and its width is defined by the QW thickness due to the high selectivity of the etching between GaAs and AlGaAs, nominally 100:1.

To reduce bulk currents, we then optimized a selective oxidation technique which allows converting the Al rich layers near the surface into a stable native oxide via the following reaction:

$$2AlAs + 6H_2O \rightarrow Al_2O_3 + As_2O_3 + 6H_2$$

This technique has been previously employed for the fabrication of nanometer-scale semiconductor islands [14], to define current apertures near the active region of quantum dots lasers [15] or to improve GaAs-based VCSELs performance by incorporating oxidation layers in order to produce high-index contrast DBR mirrors [16].

The Al-rich layers were selectively oxidized in a home-made oven consisting of a cylindrical quartz chamber embedded in a solenoid and heated by the Joule effect. A thermojunction allowed us to measure the temperature in the chamber at the sample position. The selective oxidation was driven by the continuous flow of water steam produced by nitrogen gas that bubbled deionized water. The N_2 flow and the temperature of the water source were optimized at the values of 3.3 l/min^{-1} and 80 °C, respectively. The sample was inserted in the oven few minutes after the N_2 flow started to carry aqueous vapor in the chamber in order to stabilize the temperature. The oxidation process was carried out after the selective etching and the removal of the GaAs cap layer in order to have a direct oxidation of the upper AlGaAs barrier (Fig. 1d). The temperature and oxidation time were varied from 100 to 450 °C and from 5 to 240 min, respectively.

In a next step the electrode pattern was defined by optical lithography and the electrodes were fabricated by evaporating a thin film 15 nm of Ti/Pt from a direction perpendicular to the plane of the wafer surface. As a result, an electrode gap is formed where the GaAs was removed (Fig. 1) and its size is determined (with nanometer precision) by the thickness of the GaAs QW, the thickness of deposited metal layer and by the surface roughness of the etched AlGaAs/GaAs interface due to selective etching (less than one nanometer for short etching times). We found no significant changes in etching selectivity and interface roughness after oxidation and therefore this tech-

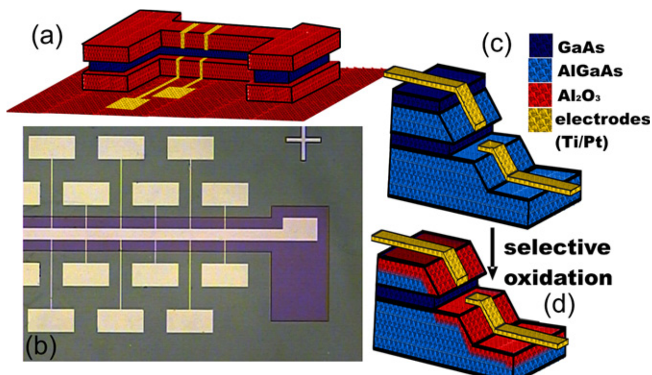

Fig. 1. (a) Schematics of the mesa nanojunctions. (b) Optical micrograph of an array of mesa nanojunctions. (c–d) Schematics of the unoxidized and oxidized nanojunctions, respectively.

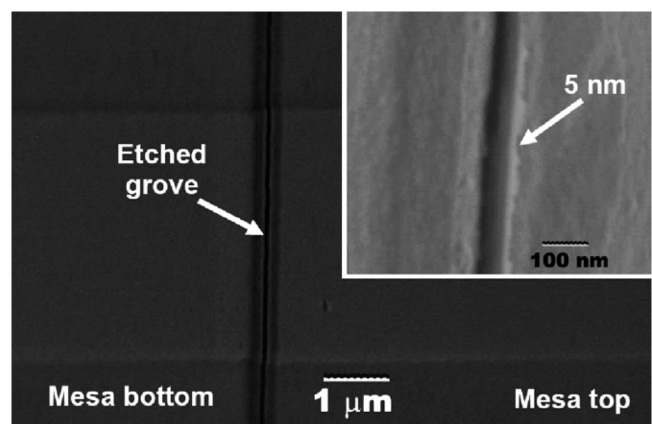

Fig. 2. SEM images of a nanojunction with a 5 nm gap fabricated on an oxidized sample. The etched grove separating the electrodes is visible in the vertical direction.

nique allowed us to fabricate nanojunctions with an electrode separation of only a few nanometers, as shown in Fig. 2. Since only photolithography is used to define the electrode pattern, this approach enables the simultaneous, economic fabrication of large arrays of nanospaced electrodes. In fact, all processes described are wafer scale, meaning that the operation or modification is performed on the entire wafer at the same time (a crucial step toward economical mass production of nanoscale devices).

3. Results and discussion

The leakage current of nanojunctions with a high Al concentration (80%) is shown in the insets of Fig. 3 as a function of the oxidation time and oxidation temperature at a fixed source-drain voltage of 1.5 V. We find that the oxidation temperature is critical and obtain as best parameters an oxidation time of 2 h at 450 °C. The open circuit leakage for various oxidation conditions is plotted on a logarithmic scale in Fig. 3. We find for all conditions an almost exponential rise in leakage current with respect of bias voltage. However, for the optimum conditions mentioned above, the leakage current remains below 30 pA up to $V_{\text{bias}} = 1.5$ V, i.e. it is reduced by six orders of magnitude as compared to unoxidized samples. Lower Al concentrations result in higher currents, due to a reduction of the oxidation rate [14]. Leakage currents in the pA range up to bias voltages of a few Volts are usually sufficient for experiments on molecules/nanoparticles and their functional devices. In such nanogaps, molecules/nanoparticles can be positioned between electrodes by electrostatic trapping or by specific immobilization procedures. This opens the way to the fabrication of complex circuits consisting of functional nanodevices.

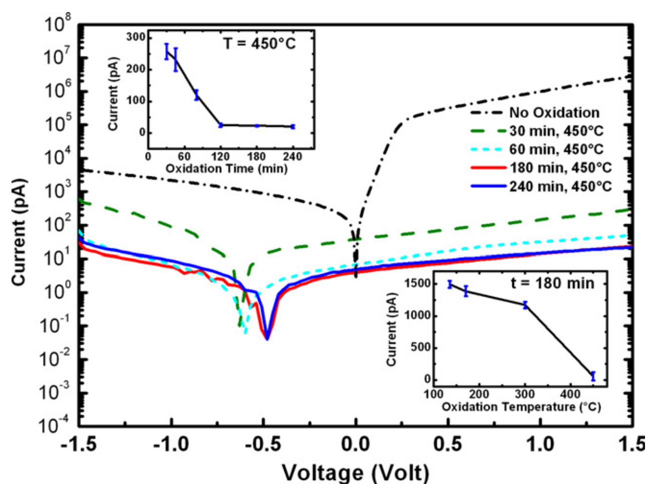

Fig. 3. Room-temperature characteristics of different oxidized nanojunctions in dark Al concentration = 80 February). By means of the selective oxidation of the AlGaAs layer the bulk open-circuit current can be reduced from tens of μA to few pA. The kink in the IV is due to log plotting near zero. Insets: Leakage current at $V_{\text{bias}} = 1.5$ V as a function of the oxidation temperature and duration.

In particular, we employed the oxidized mesa nanojunctions to investigate conduction in Azurin, a small blue-copper protein (14.6 kDa) from the bacteria *P. aeruginosa*, that – *in vitro* – is able to mediate electron transfer (ET) from cytochrome c_{551} to nitrite reductase from the same organism [17]. We are interested in Azurin because it has recently emerged as a good candidate for biomolecular electronics [7] and biosensors [18] due to the notable possibility of mediating ET and thus current flow through the redox level of its copper site. Azurin can exist in two stable electronic configurations Cu(I) and Cu(II) and its ET capability depends on the equilibrium between these two oxidation states by means of the reversible redox reaction, which converts continuously the Cu(II) copper oxidized state into the Cu(I) reduced state and *vice versa*. A disulfide bridge located at a distance of ≈2.6 nm from the copper site can be exploited for the covalent binding of Azurin on metal surfaces. Recently, a solid state biomolecular transistor, based on the ET properties of Azurin and working under ambient conditions has been demonstrated in our lab. [7] using EBL fabricated electrodes [19].

Here, our novel fabrication strategy allows us to proceed further in the demonstration and miniaturization of protein nanodevices, investigating transport in molecular tunnel junctions based on individual proteins. We immobilized Azurins in our mesa nanojunctions by cast deposition of a 20 μl drop of protein solution (1.0 mg/ml in 50 mM NH_4Ac buffer, pH 4.6), exploiting direct site-specific attachment via the disulphide bridge (RSSR). After incubation (30 min at room temperature), the buffer solution was removed and the samples were washed and then dried by high purity nitrogen flow. The width of the electrodes (defined by optical lithography) was 2–4 μm, however only in few restrictions the nanogap size matches the protein dimension. Thus, conduction through a small number of molecules in parallel is probed. Typical current–voltage characteristics

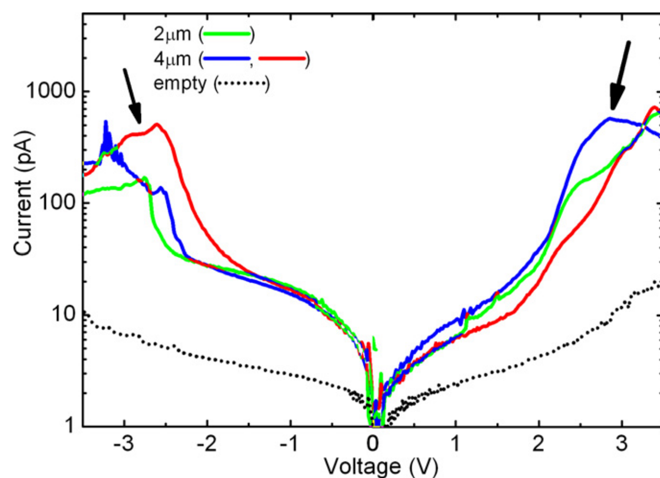

Fig. 4. Current–voltage characteristics of several mesa devices functionalized with Azurin by cast deposition of a 20 μl drop of protein solution. The black line shows the current across an empty nanojunction as a reference.

of Azurin devices are shown in Fig. 4. We observed reproducible maxima in the current (in the range ±2.2 to ±3.4 V), which mean negative differential resistance (NDR). These results are the first report of NDR in azurin devices and are in good agreement (for both current values and peak positions) with the signatures of resonant tunneling (and NDR) recently reported in metalloprotein CP-AFM junctions at the Oxford University [20].

4. Conclusions

We significantly improved the mesa-gap technique to fabricate arrays of nanojunctions by a selective oxidation process and extended thereby its applicability to room temperature. This novel mesa-gap is very interesting for molecular electronics applications where efforts towards mass production and strategies for the fabrication of large arrays of single-molecule components into molecular-scale electronic circuits are needed. Transport in Azurin was also investigated using these nanojunctions under ambient conditions with typical molecular features (such as NDR) observed in the *I–V* characteristics.

Acknowledgements

The authors gratefully acknowledge the support by the SAMBA and SpiDME European project, the IIT and the Italian MIUR (FIRB Molecular Nanodevices). Moreover, we would like to thank Marco Zanella, Teresa Todaro and Vittorianna Tasco for fruitful discussions and providing materials, and Eliana D'Amone for technical assistance.

References

[1] G. Maruccio, R. Cingolani, R. Rinaldi, Journal Of Materials Chemistry 14 (2004) 542.
[2] S.J. Tans, A.R.M. Verschueren, C. Dekker, Nature 393 (1998) 49.
[3] J. Park, A.N. Pasupathy, J.I. Goldsmith, et al., Nature 417 (2002) 722.
[4] A. Bachtold, P. Hadley, T. Nakanishi, et al., Science 294 (2001) 1317.
[5] Y. Huang, X.F. Duan, Y. Cui, et al., Science 294 (2001) 1313.
[6] G. Maruccio, P. Visconti, V. Arima, et al., Nanoletters 3 (2003) 479.
[7] G. Maruccio, A. Biasco, P. Visconti, et al., Advanced Materials 17 (2005) 816.
[8] J.G. Kushmerick, D.B. Holt, J.C. Yang, et al., Physical Review Letters 89 (2002) 086802.
[9] R.M. Metzger, B. Chen, U. Hopfner, et al., Journal Of The American Chemical Society 119 (1997) 10455.
[10] J. Chen, M.A. Reed, A.M. Rawlett, et al., Science 286 (1999) 1550.
[11] A.N. Pasupathy, R.C. Bialczak, J. Martinek, et al., Science 306 (2004) 86.
[12] W.J. Liang, M.P. Shores, M. Bockrath, et al., Nature 417 (2002) 725.
[13] R. Krahne, A. Yacoby, H. Shtrikman, et al., Applied Physics Letters 81 (2002) 730.
[14] M. De Vittorio, M.T. Todaro, V. Vitale, et al., Microelectronic Engineering 61–62 (2002) 651.
[15] A. Fiore, J.X. Chen, M. Ilegems, Applied Physics Letters 81 (2002) 1756.
[16] M.H. Macdougal, P.D. Dapkus, V. Pudikov, et al., IEEE Photonics Technology Letters 7 (1995) 229.
[17] E. Vijgenboom, J.E. Busch, G.W. Canters, Microbiology-Uk 143 (1997) 2853.
[18] G. Gilardi, T. Den Blaauwen, G.W. Canters, Journal of Controlled Release 29 (1998) 231.
[19] G. Maruccio, P. Visconti, S. D'Amico, et al., Microelectronic Engineering 67–68 (2003) 838.
[20] J.J. Davis, D.A. Morgan, C.L. Wrathmell, et al., Journal Of Materials Chemistry 15 (2005) 2160.